Journal of the American Pomological Society 80(4): 89-98 2026. https://doi.org/10.71318/ 70k4mt72.

UAV Multispectral Imagery for Assessing Tree Health in Tart Cherry Orchards with a Focus on Powdery Mildew Detection

Christina Lilligren[1], Kurt Wedegaertner[1], Marion Murray[2], Brent Black[1], Anderson Safre[3], Alfonso Torres-Rua[4]

Additional index words: Tart cherry, powdery mildew, UAV multispectral imagery

Abstract

Unmanned aerial vehicle (UAV)-based multispectral imagery could provide a more efficient approach to pest scouting in tart cherry, a relatively low-input orchard crop. We evaluated whether vegetation indices derived from UAV-mounted multispectral imagery could detect powdery mildew (PM) in three commercial tart cherry orchard blocks in Utah during 2022 and 2023. Powdery mildew severity was surveyed repeatedly and compared with vegetation indices calculated from multispectral imagery collected during the same period. The optimized chlorophyll vegetation index (OCVI) showed the strongest overall relationship with PM severity, but correlations were only moderate when data were pooled across orchards and dates. Within individual orchards and sampling dates, vegetation indices were not consistently related to PM severity. Relationships were especially weak when analyses were restricted to observations below an estimated economic threshold of 20% severity, where early detection would be most useful for management decisions. Although UAV multispectral imagery was not reliable for early PM detection, it was useful for identifying broader spatial variability in tree health. Tree health, assessed using red-edge normalized difference vegetation index as an indicator of canopy chlorosis and vigor, varied substantially among orchards and was associated with canopy density and apparent soil electrical conductivity (ECa). In the most variable orchard, poorer tree health and greater chlorosis were concentrated in areas of lower canopy density and higher ECa, corresponding to finer-textured soils. These findings indicate that UAV multispectral imagery was not reliable for early detection of PM in tart cherry under commercial orchard conditions but was useful for characterizing orchard-scale variability in tree health related to canopy structure and soil properties.

Introduction

Tart cherry (*Prunus cerasus* L.) is an economically important fruit crop in Utah, which ranked second nationally in production behind Michigan from 2020 to 2022 and accounted for an average of 15% of total U.S. tart cherry production during that period (USDA 2024). Utah orchards produce higher yields per hectare than those in Michigan, averaging 14.0 $Mg \cdot ha^{-1}$ over the past decade compared with 7.9 $Mg \cdot ha^{-1}$ in Michigan (Bardenhagen 2022). Despite its importance, tart cherry is a relatively low-value crop, with a 2022 price of $0.73/kg compared with $3.59/kg for sweet cherry (USDA 2023). This lower crop value requires reduced labor inputs, creating a need for efficient methods to monitor pest severity.

Powdery mildew (PM), caused by *Podosphaera cerasi*, can reduce tart cherry productivity and vigor and is a promising target for remote assessment because symptoms occur on foliage throughout the canopy (Lilligren et al. 2023; Murray et al. 2025). The pathogen overwinters as chasmothecia in leaf litter and bark crevices, and spring infection occurs when moisture is present and temperatures exceed 10 °C (Grove and Boal 1991a). Visible colonies typically develop four to six weeks after bud break, and secondary infections may continue through much of the growing season (Grove and

[1]Department of Plants, Soils and Climate, Utah State University, 4820 Old Main Hill, Logan, UT 84322, USA
[2]Department of Biology, Utah State University, 5305 Old Main Hill, Logan, UT, 84322
[3]Division of Agricultural and Natural Resources, University of California, Parlier CA 93648, USA
[4]Department of Civil and Environmental Engineering, Utah State University, 4110 Old Main Hill, Logan, UT 84322, USA
This is an open access article distributed under the CC BY-NC license (https://creativecommons.org/licenses/by-nc/4.0/).

Boal 1991b; Grove and Boal 1991c; Schmidt-Jeffris et al. 2019; Utah State University 2024). Because successful management depends on timely detection, an efficient scouting method for early PM development would be valuable. Because initial outbreaks can show dramatic spatial variability, remote detection could facilitate more efficient control strategies including targeted or variable rate applications of crop protectants. Although comparable Utah-specific production budgets are not available, crop protection in a 2022 Michigan tart cherry production budget was estimated at approximately $407/acre, representing about 13% of total production costs (Bardenhagen et al. 2022). The Michigan production system and pest complex differ from those in Utah, and these costs are not specific to powdery mildew, but they illustrate that crop protection represents a meaningful production expense. Targeting affected areas rather than treating entire orchard blocks could reduce pesticide use and associated application costs. In this study, PM was used as a test case for evaluating whether UAV multispectral imagery could identify pest-related spatial variability at a scale useful for targeted orchard management.

Powdery mildew infection can alter leaf reflectance in spectral bands associated with chlorophyll and canopy stress, including the red-edge and near-infrared regions (Chandel et al. 2021). Similar responses have been reported in other crops, where PM infection altered carbohydrate composition, reduced photosynthesis, and affected pigment concentrations (Abood 2003; Ellis et al. 1981; Percival and Fraser 2002). Multispectral imaging has also been used to detect disease damage in wheat, opium poppy, orange, pear, and apple (Calderón et al. 2014; Chandel et al. 2020; Chandel et al. 2021; DadrasJavan et al. 2019; Kumar et al. 2012; Lan et al. 2020; Su et al. 2018; Schoofs et al. 2020). However, little information is available on the use of UAV-based multispectral imagery to detect PM in tart cherry under commercial orchard conditions. Therefore, the objective of this study was to determine whether vegetation indices derived from UAV-mounted multispectral imagery could detect PM severity in tart cherry at commercially relevant management thresholds.

Materials and Methods

Orchard sites and sampling design. Field studies were conducted in commercial tart cherry orchards in Utah during 2022 and 2023. Preliminary surveys in 2022 were conducted in four orchards in southern Utah County, selected for a history of spatial variability in pest presence. Forty trees were surveyed weekly for PM, and four unmanned aerial vehicle (UAV) flights were completed during the survey period. Because the 2022 sample size was insufficient to provide meaningful relationships between pest severity and multispectral imagery, those observations were used only to refine field sampling and disease quantification methods for 2023.

The primary study was conducted in 2023 in three commercial tart cherry orchard blocks in Utah: Orchard S and Orchard H in southern Utah County, and Orchard T in Box Elder County. Orchard blocks were again selected based on a history of spatially variable PM severity. Two transects were established in each orchard to represent the range of disease history. In two orchards, every second tree along each transect was surveyed, for totals of 43 and 40 trees, respectively. In the third orchard, every fourth tree was surveyed because of longer rows, for a total of 55 trees.

Powdery mildew assessment. Powdery mildew was assessed weekly from 27 May through 5 July 2023. Ten leaves per tree were collected at random from actively growing shoots in the lower, middle, and upper canopy. The sampling intensity was consistent with commercial tart cherry scouting guidance recommending evaluation of 10 terminals per tree for powdery mildew assessment (Ontario Ministry of Agriculture, Food, and Agribusiness 2026). Each leaf was visually rated for percent PM coverage using methods adapted from published studies in other crops (Calabro et al. 2009; Grove et al. 2000). To improve consistency among surveyors, a standard area diagram was used to guide disease severity estimates. Ratings from 0 to 100% were averaged across the 10 sampled leaves to obtain a weekly PM severity value for each tree.

Leaf-level spectral reflectance. Spectroradiometry observations were conducted to determine whether PM infection produced a detectable leaf-level spectral response within wavelengths corresponding to the multispectral bands used for UAV imaging. This analysis was intended to determine whether a spectral signal associated with PM was present at the leaf scale before evaluating whether that signal could be detected at the whole-canopy scale using UAV imagery.

Ten healthy leaves and eight leaves with PM colonies less than 10 mm in diameter were selected by two experienced surveyors using a 10× hand lens. Reflectance was measured from 400 to 999.5 nm in 0.5-nm increments in the laboratory (BLUE-Wave Spectrometer, StellarNet, Tampa, FL, USA). For each leaf, reflectance measurements were averaged within wavelength ranges corresponding to the Altum-PT multispectral camera (AgEagle Aerial Systems, Wichita, KS, USA) bands.

Multispectral imaging. Multispectral images were collected every two to three weeks from 8 June through 14 Sept. 2023 using an Altum-PT multispectral camera mounted on a DJI Matrice 300 RTK UAV (DJI Technology, Shenzhen, China) flown at 120 m altitude (Chandel et al. 2021; Luedeling et al. 2009). Five ground control points were used to improve positional accuracy. Images were processed in Agisoft Metashape professional v.2.0.3 (Agisoft, LLC, St. Petersburg, Russia) to generate orthomosaics and elevation models. Canopy reflectance values for red, green, blue, red-edge, and near-infrared bands were extracted for each surveyed tree, and vegetation indices were calculated and compared with PM severity (Xiao et al. 2022). Tree health was assessed using red-edge normalized difference vegetation index (RNDVI) as an indicator of canopy chlorosis and vigor. Lower RNDVI values were interpreted as reduced chlorophyll content and poorer tree health, whereas higher values indicated healthier canopies (Main et al. 2011).

Canopy density. Canopy density was estimated from ceptometry-based light interception measurements collected on 6 June, 23 June, and 12 July 2023, representing early, middle, and late stages of tart cherry fruit and PM development. Measurements were collected along both sampled transects in each orchard as described by Wedegaertner et al. (2026). Fifteen 30-cm light bar sensors (Apogee SQ-311, Apogee Instruments, Logan, UT, USA) mounted on a boom attached to an all-terrain vehicle recorded under-canopy light and GPS measurements every second as the vehicle passed along both sides of the sampled transects. A reference sensor located outside the canopy simultaneously recorded unobstructed light. Light interception was calculated by comparing under-canopy and unobstructed light measurements, and spatial maps were generated in ArcGIS Pro using kriging. For each surveyed tree, light interception values were averaged for the tree and the surrounding 10-m area to represent local canopy density.

Soil characterization. Apparent soil electrical conductivity (ECa) was measured using an EM38-MK2 conductivity meter towed through orchard alleyways at 12 to 14 $km \cdot h^{-1}$ in spring, when soil moisture was assumed to be relatively uniform. One-second mean ECa values were recorded with corresponding GPS coordinates. Soil samples collected across the ECa range were used for particle size analysis by the hydrometer method, and ECa values were interpolated in ArcGIS Pro using ordinary kriging with a spherical model (Heil and Schmidhalter 2015; Knotters et al. 1995). For each surveyed tree, mean ECa within a 2.5-m radius was used to represent local soil characteristics.

Statistical analysis. Relationships between PM severity and vegetation indices were evaluated using simple linear regression in Python v3.10.16 with the statsmodels package (Python Software Foundation, Wilmington, DE, USA). Analyses were conducted using pooled data across orchards and dates, as well as separately within individual orchards and sampling dates, to determine whether relationships observed in the combined dataset were consistent under commercial field conditions. Additional regression analysis was conducted for observations below an estimated economic threshold of 20% PM severity. Relationships between

ECa and canopy density were evaluated using simple linear regression separately for each orchard. Leaf-level reflectance was compared between healthy and infected leaves within each multispectral band using Welch's two-sample t-tests with Holm adjustment for multiple comparisons. Statistical significance was assessed at $p \leq 0.05$.

Results and Discussion

Leaf-level spectral reflectance. At the individual leaf scale, PM infection altered tart cherry leaf reflectance. Mean reflectance of infected leaves was greater than that of healthy leaves, with the largest differences observed in the red-edge and near-infrared regions (Fig. 1). Relative to healthy leaves, infected leaves had reflectance values that were 3.4 percentage points higher in the red-edge band and 3.3 percentage points higher in the near-infrared band. Differences between healthy and infected leaves were significant in the blue, green, red, and red-edge bands (Holm-adjusted p-values < 0.001, 0.024, 0.045, and 0.028, respectively), but not in the near-infrared band (Holm adjusted p = 0.148).

Powdery mildew progression and pooled vegetation index relationships. Powdery mildew severity increased during the 2023 sampling period in all three orchard blocks. Mean PM severity increased from 14 to 39% in Orchard S, from 27 to 58% in Orchard H, and from 16 to 60% in Orchard T between 6 June and 27 June 2023. When PM severity was compared with vegetation indices derived from UAV multispectral imagery, the strongest pooled relationships across orchards and dates were observed for optimized chlorophyll vegetation index (OCVI) and chlorophyll vegetation index (CVI), with R^2 values of 0.414 and 0.413, respectively (Fig. 2).

The pooled relationships, however, were not consistent within individual orchards and sampling dates. When data were stratified by orchard and date, none of the within-orchard relationships between vegetation indices and PM severity were statistically significant (Fig. 3). This pattern suggests that the pooled correlations were influenced partly by differences among orchards and seasonal changes in canopy reflectance, rather than by PM severity alone. Thus, the leaf-level disease signal was not expressed reliably at the orchard scale under commercial conditions.

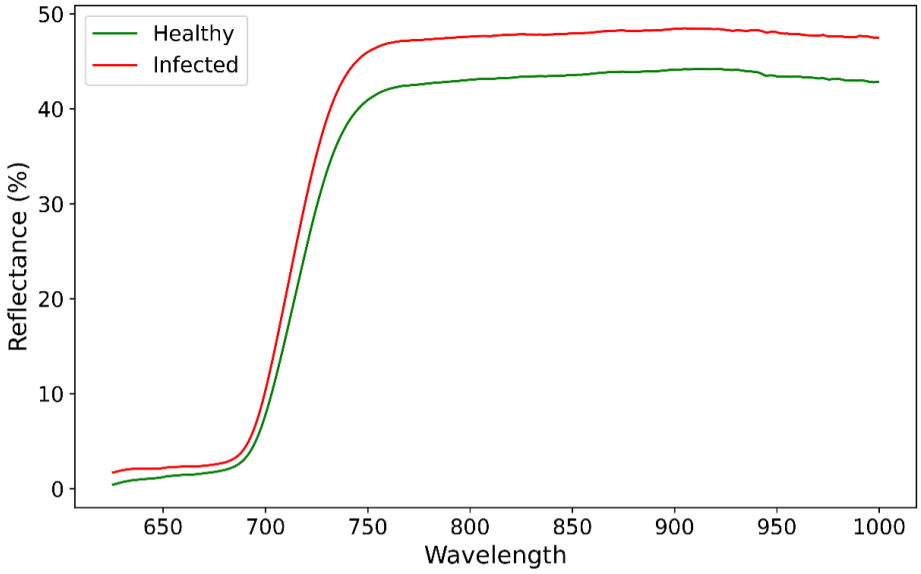


Fig. 1. Reflectance spectrum of healthy and powdery mildew-infected leaves of 'Montmorency' tart cherry. Values represent mean reflectance of 10 healthy leaves and 8 infected leaves. Mean reflectance in the red-edge and near-infrared spectral regions was greater in infected leaves.

These results indicated that PM altered tart cherry leaf reflectance in spectral regions commonly used in multispectral image analysis.

Although an economic injury level for pow-

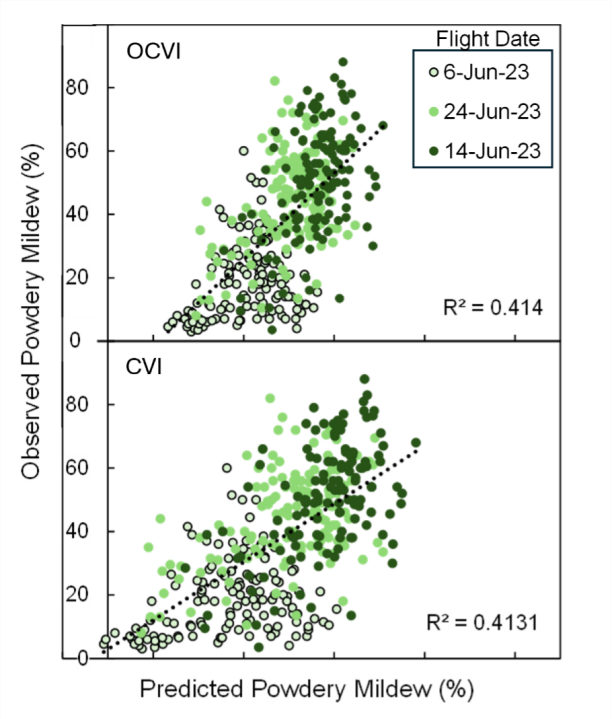


Fig. 2. Relationships between observed powdery mildew severity and powdery mildew severity predicted from the two best-performing vegetation indices using pooled data across orchards and sampling dates in 2023. Top: model based on optimized chlorophyll vegetation index (OCVI); bottom: model based on chlorophyll vegetation index (CVI). Point colors indicate UAV flight date.

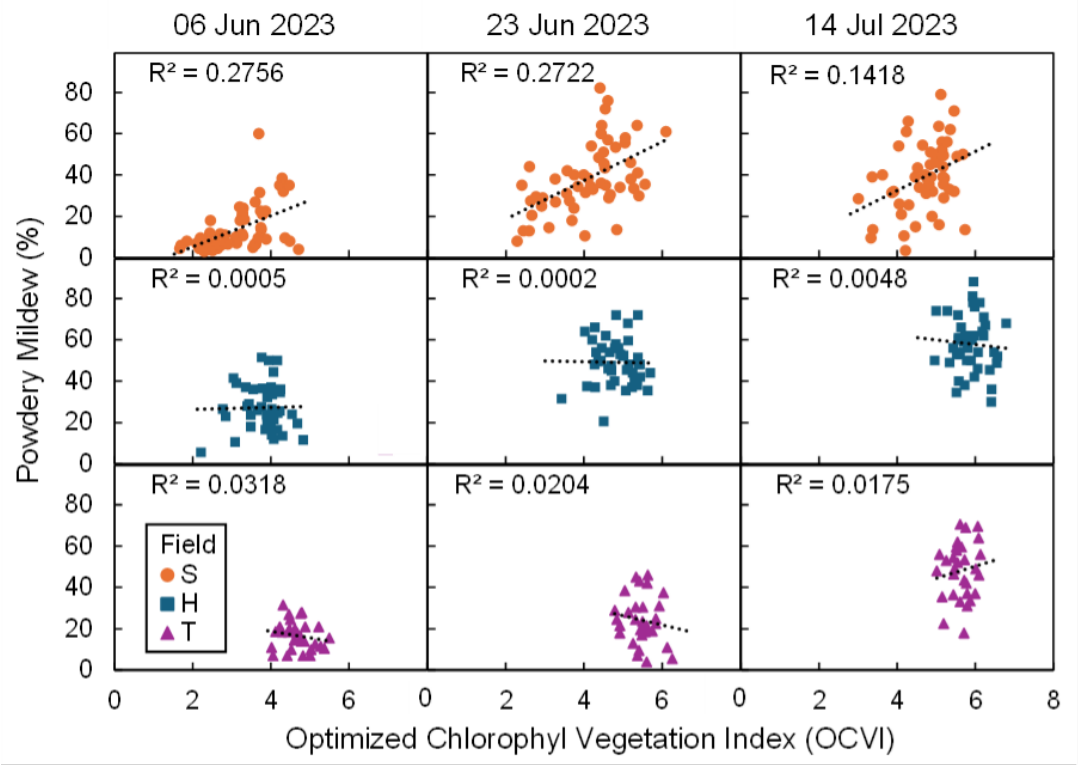


Fig. 3. Relationship between powdery mildew severity and optimized chlorophyll vegetation index (OCVI) for three tart cherry orchard blocks on 6 June, 23 June, and 14 July 2023. Relationships within individual orchard blocks and sampling dates were not statistically significant. Multispectral imagery was collected within 10 d of powdery mildew assessment.

dery mildew on tart cherry does not exist, the authors used a value of 20% canopy infestation for statistical purposes based on Yoder & Hickey's 1995 paper that suggests management adjustment for apple powdery mildew before 20% severity. Of the 590 PM observations collected across orchards and dates, only 25% were below this 20% threshold, and most of these occurred during the first two weeks of sampling. When observations below 20% PM severity alone were analyzed, the relationship between OCVI and PM was weak (R^2 = 0.22). UAV multispectral imagery therefore did not reliably detect PM at the levels most relevant to potential economic injury or management decision. This agrees with prior work in apple, where multispectral detection of PM was more successful only after infection had become visually obvious (Chandel et al. 2021).

Although PM-related differences in leaf reflectance were detectable at the individual-leaf scale, those differences did not translate into reliable orchard-scale detection using UAV multispectral imagery under commercial conditions. The contrast between the leaf-level and orchard-scale results suggests several likely limitations. Early PM colonies occupied only a small portion of total leaf area, so their spectral contribution may have been too weak to influence canopy-scale vegetation indices. In addition, the large three-dimensional canopy structure of tart cherry may have obscured infected leaves from aerial view, particularly in the middle and lower canopy. Orchard-level variation in chlorophyll content, canopy development, and lighting conditions may also have overwhelmed the spectral response associated with early PM infection. Together, these factors likely explain why PM-related reflectance differences were detectable on individual leaves but were not translated into reliable UAV-based detection at commercially useful thresholds. Ground-truth sampling may also have contributed to uncertainty in these relationships. Although the sampling intensity was based on commercial scouting recommendations, powdery mildew can be unevenly distributed within the large three-dimensional canopy, and sampling 10 leaves may not fully represent whole-tree disease severity, particularly when disease severity is low.

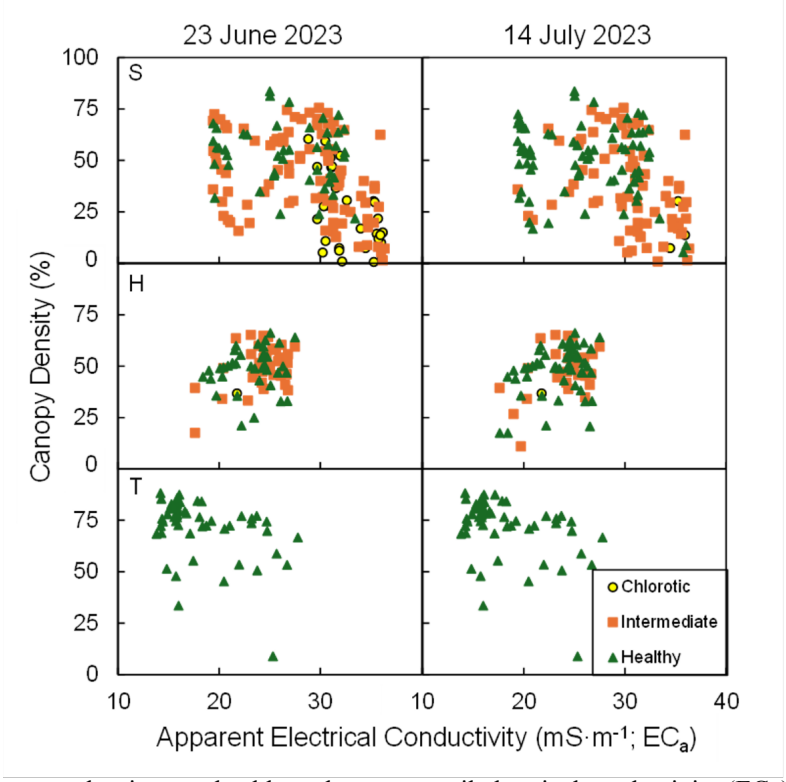


Fig. 4. Relationship among canopy density, tree health, and apparent soil electrical conductivity (ECa) across orchard blocks. Tree health was assessed using red-edge normalized difference vegetation index (RNDVI) as an indicator of canopy chlorosis and vigor. In Orchard S, most chlorotic trees occurred in areas with higher ECa, corresponding to finer-textured soils.

Under the conditions of this study, UAV multispectral imagery was not a reliable tool for early PM detection in tart cherry orchards.

Spatial variability in tree health, canopy density, and soil properties. Although UAV multispectral imagery was not reliable for early PM detection, it was useful for identifying broader spatial variability in tart cherry tree health. Tree health, assessed using RNDVI as an indicator of canopy chlorosis and vigor, varied substantially among orchards. Orchard S showed the greatest variability, with RNDVI values ranging from 0.19 to 0.54 and an average of 0.42 across the season. Orchard H was intermediate in variability, with RNDVI values ranging from 0.27 to 0.54 and averaging 0.45, whereas Orchard T was the most uniform, with all RNDVI values above 0.50 and no visible chlorosis symptoms.

In Orchard S, poorer tree health was associated with higher ECa and lower canopy density (Fig. 4). Canopy density was negatively related to ECa in Orchard S ($R^2 = 0.20$, $p < 0.001$). However, the direction of this relationship differed among orchards. Orchard H showed a positive relationship between ECa and canopy density ($R^2 = 0.18$, $p < 0.001$), whereas Orchard T showed a weaker negative relationship ($R^2 = 0.13$, $p = 0.005$). These results indicate that relationships between ECa and canopy density were orchard-specific. The differing directions of these relationships likely reflect differences in soil properties and orchard conditions among sites, as ECa is influenced by soil characteristics including texture and water-holding conditions. Most chlorotic trees occurred where ECa exceeded 30 $mS \cdot m^{-1}$, corresponding to finer-textured soils (high clay content). In contrast, the healthiest and most vigorous trees in Orchard S were located in areas with lower ECa values associated with coarser soil. These results suggest that spatial variation in soil properties contributed to differences in tree health within the orchard.

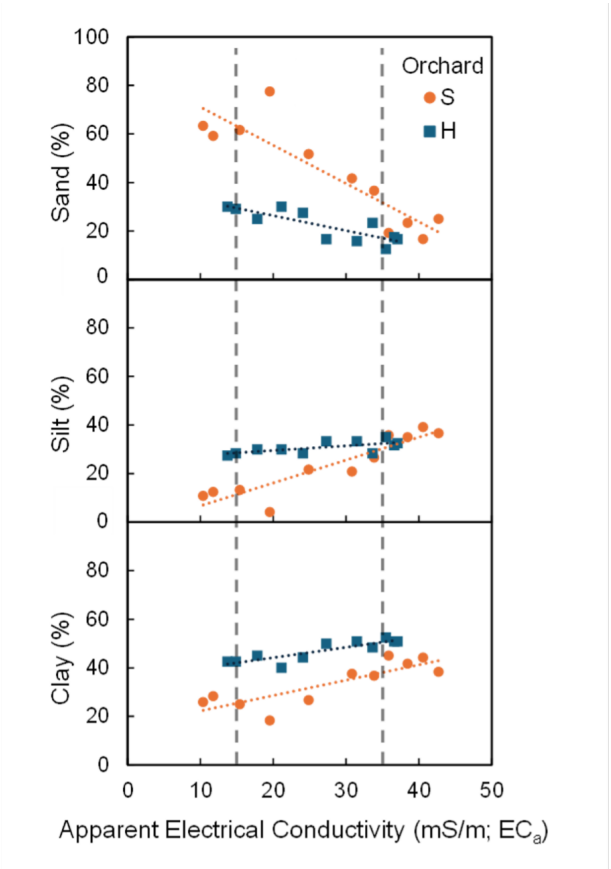


Fig. 5. Relationship between apparent soil electrical conductivity (ECa) and soil texture components based on 11 soil samples collected from locations representing predetermined ECa percentiles. Higher ECa values were associated with lower sand content and higher silt and clay content.

The relationship between ECa and soil texture supported this interpretation. Across the 11 soil samples collected from predetermined ECa percentiles, higher ECa values were associated with lower sand content and higher silt and clay content (Fig. 5). Thus, ECa provided a useful indicator of soil texture variation within orchards. In Orchard S, areas with higher ECa were associated with reduced tree vigor and greater chlorosis, suggesting that finer-textured soils may have contributed to poorer drainage, root stress, and greater risk of Phytophthora root rot (Stern et al. 1977), which was observed in some trees. Similar associations between ECa and orchard performance have been reported previously, although the direction of the relationship can vary among sites depending on soil properties and growing conditions (Corwin and Lesch 2005; Wedegaertner et al. 2026).

In Orchard S, trees with lower PM severity on 20 June 2023 were more frequently located in areas with relatively high ECa values (≥30 $mS \cdot m^{-1}$) (Fig. 6). Because these same areas also had lower canopy density and poorer tree health, this pattern likely reflected reduced canopy development rather than a direct effect of soil conditions on PM.

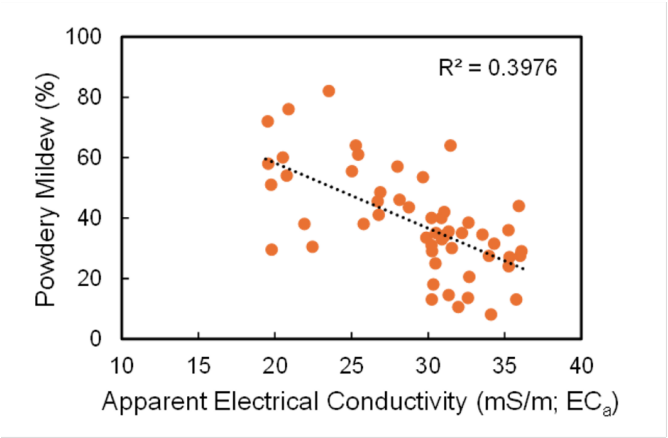


Fig. 6. Relationship between powdery mildew severity surveyed on 20 June 2023 and apparent soil electrical conductivity (ECa) in Orchard S. Trees with lower PM severity were more frequently located in areas with ECa greater than or equal to 30 $mS \cdot m^{-1}$, likely reflecting indirect effects of lower canopy density and reduced vigor in finer-textured soils.

Orchard H showed intermediate RNDVI, ECa, and canopy density, whereas Orchard T was comparatively uniform in all three measures. Together, these orchard differences support the interpretation that soil-related spatial heterogeneity contributed to variation in tree health and canopy development across sites.

Although UAV multispectral imagery did not reliably detect PM severity, the combined spatial datasets were useful for identifying orchard zones that differed in vigor, canopy structure, and apparent soil texture.

Conclusion

Powdery mildew infection altered tart cherry leaf reflectance in spectral regions commonly used in multispectral image analysis, but these leaf-level differences did not translate into reliable orchard-scale detection using UAV imagery under commercial conditions. Relationships between vegetation indices and PM severity were only moderate when data were pooled and were not significant within individual orchards and sampling dates. Detection was especially weak below our estimated economic threshold of 20% severity. However, UAV multispectral imagery was useful for identifying broader spatial variability in tree health. In the most spatially variable orchard, poorer canopy vigor and greater chlorosis occurred more frequently in areas with lower canopy density and higher ECa. However, relationships between ECa and canopy density were significant in all three orchards but differed in direction, with negative relationships in Orchards S and T and a positive relationship in Orchard H. This indicates that associations between soil-related variability and canopy development were orchard-specific rather than consistent across sites. Because ECa and soil texture cannot be readily modified in established orchards, identifying these spatial patterns may help inform site-specific irrigation management and could also be useful for pre-plant planning and soil amendment strategies. These findings indicate that currently available UAV multispectral approaches have limited value for management-timed PM scouting in tart cherry, although improvements in sensor resolution or canopy-specific imaging approaches may increase future utility.

Acknowledgements

This research was supported by the U.S. Department of Agriculture National Institute of Food and Agriculture Specialty Crop Research Initiative (USDA NIFA-SCRI) under grant no. 2021-51181-35868, and by a USDA National Needs Fellowship. Additional support was provided by the Utah Agricultural Experiment Station, Utah State University, and approved as journal paper no. 9998. The authors thank Kylara Barney of Payson Fruit Growers for technical assistance, and we also thank Valley View Orchards and Thorne Orchards for providing orchard access and cooperating in the implementation of this research.

Literature Cited

Abood JK, Lösel DM. 2003. Changes in carbohydrate composition of cucumber leaves during the development of PM infection. Plant Pathol. 52:256-265. https://doi.org/10.1046/j.1365-3059.2003.00814.x.

Bardenhagen C, Rothwell N, Colella F, Nugent J. 2022. Michigan tart cherry cost of production study 2022. Mich Agric Ext Bull. E3474.

Calabro JM, Spotts RA, Grove GG. 2009. Effect

of training system, rootstock, and cultivar on sweet cherry PM foliar infections. HortScience. 44:481-482. https://doi.org/10.21273/HORTSCI.44.2.481.

Calderón R, Montes-Borrego M, Landa BB, Navas-Cortés JA, Zarco-Tejada PJ. 2014. Detection of downy mildew of opium poppy using high-resolution multispectral and thermal imagery acquired with an unmanned aerial vehicle. Precision Agric. 15:639-661. https://doi.org/10.1007/s11119-014-9360-y.

Chandel AK, Khot LR, Sallato B. 2020. Towards rapid detection and mapping of PM in apple orchards, p 288-292. In: 2020 IEEE International Workshop on Metrology for Agriculture and Forestry (MetroAgriFor). https://doi.org/10.1109/MetroAgriFor50201.2020.9277544.

Chandel AK, Khot LR, Sallato B. 2021. Apple PM infestation detection and mapping using high-resolution visible and multispectral aerial imaging technique. Sci Hortic. 287:110228. https://doi.org/10.1016/j.scienta.2021.110228.

DadrasJavan F, Samadzadegan F, Pourazar SHS, Fazeli H. 2019. UAV-based multispectral imagery for fast citrus greening detection. J Plant Dis Prot. 126:307-318. https://doi.org/10.1007/s41348-019-00234-8.

Ellis M, Ferree D, Spring D. 1981. Photosynthesis, transpiration, and carbohydrate content of apple leaves infected by *Podosphaera leucotricha.* Phytopathol. 71:392-395.

Grove GG, Boal RJ. 1991a. Overwinter survival of *Podosphaera clandestina* in eastern Washington. Phytopathol. 81:385-391.

Grove GG, Boal RJ. 1991b. PM of sweet cherry: influence of temperature and wetness duration on release and germination of ascospores of *Podosphaera clandestina*. Phytopathol. 81:1271-1275.

Grove GG, Boal RJ. 1991c. Factors affecting germination of conidia of *Podosphaera clandestina* on leaves and fruit of sweet cherry. Phytopathol. 81:1513-1518.

Grove GG, Boal RJ, Bennett LH. 2000. Managing PM of cherry in Washington orchards and nurseries with spray oils. Plant Health Prog. 1:2. https://doi.org/10.1094/PHP-2000-0728-01-RS.

Kumar A, Lee WS, Ehsani R, Albrigo G, Yang C, Mangan RL. 2012. Citrus greening disease detection using aerial hyperspectral and multispectral imaging techniques. J Appl Remote Sens. 6:063542. https://doi.org/10.1117/1.JRS.6.063542.

Lan Y, Huang Z, Deng X, Zhu Z, Huang H, Zheng Z, Tong Z. 2020. Comparison of machine learning methods for citrus greening detection on UAV multispectral images. Comput Electron Agric. 171:105234. https://doi.org/10.1016/j.compag.2020.105234.

Lilligren C, Murray M, Black B, Torres-Rua A, Wedegaertner K, Safre A, Papenfuss K. 2023. Precision agriculture techniques for evaluating tart cherry tree health. In: II International Symposium on Precision Management of Orchards and Vineyards. Acta Hortic. 1395:197-200. https://doi.org/10.17660/ActaHortic.2024.1395.26.

Luedeling E, Hale A, Zhang M, Bentley WJ, Dharmasri CL. 2009. Remote sensing of spider mite damage in California peach orchards. Int J Appl Earth Obs Geoinf. 11:244-255. https://doi.org/10.1016/j.jag.2009.03.002

Main R, Cho MA, Mathieu R, O'Kennedy MM, Ramoelo A, Koch S. 2011. An investigation into robust spectral indices for leaf chlorophyll estimation. ISPRS J Photogrammetry Remote Sens. 66:751-761. https://doi.org/10.1016/j.isprsjprs.2011.08.001

Murray M, Lilligren C, Kast M. 2025. Cherry powdery mildew in Utah. Utah State University Extension Plant Health. https://extension.usu.edu/planthealth/research/cherry-powdery-mildew-in-utah.

Ontario Ministry of Agriculture, Food and Agribusiness. 2026. Powdery mildew: Tart cherries. Ontario Crop Protection Hub. https://cropipm.omafra.gov.on.ca/en-ca/crops/tart-cherries/diseases/4d8c8b67-eb4a-4112-8b13-87e65d129fb8#identification. [accessed 25 Sept. 2026].

Percival GC, Fraser GA. 2002. The influence of PM infection on photosynthesis, chlorophyll

fluorescence, leaf chlorophyll and carotenoid content of three woody plant species. Arboric J. 26:333-346. https://doi.org/10.1080/03071375.2002.9747348.

Schmidt-Jeffris RA, Beers EH, Duso C. 2019. Integrated management of mite pests of tree fruit, p. 425-452. In: Xu X, Fountain M (eds). Integrated management of diseases and insect pests of tree fruit. Burleigh Dodds Science Publishing, London, UK.

Schoofs H, Delalieux S, Deckers T, Bylemans D. 2020. Fire blight monitoring in pear orchards by unmanned airborne vehicles (UAV) systems carrying spectral sensors. Agron. 10:615. https://doi.org/10.3390/agronomy10050615.

Stern RE, Zentmyer GA, Kaufmann MR. 1977. The influence of matric potential, soil texture, and soil amendment on root disease caused by *Phytophthora cinnamomi*. Phytopathol. 67: 1495-1500.

Su J, Liu C, Coombes M, Hu X, Wang C, Xu X, Li Q, Guo L, Chen W-H. 2018. Wheat yellow rust monitoring by learning from multispectral UAV aerial imagery. Comput Electron Agric. 155:157-166.

United States Department of Agriculture, National Agricultural Statistics Service. 2023. Noncitrus fruits and nuts 2022 summary. USDA. 87 p.

United States Department of Agriculture, National Agricultural Statistics Service. 2024. Census of Agriculture. USDA.

Utah State University. 2024. PM. USU. https://extension.usu.edu/planthealth/ipm/notes_orn/list-flowers/powdery-mildew. [accessed 9 Oct. 2024].

Wedegaertner K, Black B, Safre A, Torres-Rua A, Cardon G, Yost M. 2026. Integrating soil and canopy sensing to map and relate variability in tart cherry orchards. Precision Agric. 27:136. https://doi.org/10.1007/s11119-026-10436-4.

Xiao D, Pan Y, Feng J, Yin J, Liu Y, He L. 2022. Remote sensing detection algorithm for apple fire blight based on UAV multispectral image. Comput Electron Agric. 199:107137.

Yoder, K. S., and Hickey, K. D. 1995. Apple powdery mildew. in: Mid-Atlantic Orchard Monitoring Guide. H. W. Hogmire, eds. Northeast Regional Agricultural Engineering Department, Ithaca, NY.